

Inhibition effect of Ilex kudingcha C.J. Tseng (Kudingcha) extract on J55 Steel in 3.5wt% NaCl Solution Saturated with CO₂

Songsong Chen³, Ambrish Singh³, Yuanluqi Wang³, Wanying Liu³, Kuanhai Deng², Yuanhua Lin^{1,2,3,*}

¹ State Key Laboratory of Oil and Gas Reservoir Geology and Exploitation, Southwest Petroleum University, Chengdu 610500, Sichuan, China

² CNPC Key Lab for Tubular Goods Engineering, Southwest Petroleum University, Chengdu 610500, Sichuan, China

³ School of Materials Science and Engineering, Southwest Petroleum University, Chengdu, Sichuan 610500, China.

*E-mail: yhlin28@163.com

Received: 11 September 2016 / *Accepted:* 20 November 2016 / *Published:* 12 December 2016

The corrosion effect on J55 steel in 3.5wt% NaCl solution saturated with CO₂ by ethanol extract of Ilex kudingcha C.J. Tseng (KDC) leaves has been studied using fourier transform infrared spectroscopy (FTIR), potentiodynamic polarization, electrochemical impedance spectroscopy (EIS) and scanning electron microscopy (SEM) methods. The results showed that KDC can be used as a good green inhibitor in the test solution. Inhibition efficiency increases with increasing the inhibitor concentration and KDC extract act as a mixed-type inhibitor. Adsorption behavior of the KDC extracts on J55 steel surface is also studied by Langmuir, Frumkin and Temkin isotherms and the data fitting results suggested that Langmuir isotherm model is the most suitable adsorption model.

Keywords: Corrosion inhibition; J55 steel; Adsorption isotherm; Electrochemical study

1. INTRODUCTION

In nature, except the precious metals, most of the pure metals and alloys stay in a thermodynamic instability, they could interact with corrosive medium to form metal compounds and tend to have reached a stable state [1,2]. Metal corrosion problem exists in almost all industries, for example, energy [3], transportation [4], aerospace [5], ocean development [6] etc. The corrosion problem is particularly in the oil and gas industry, because in the oil and gas exploration and transferring process, the existence of water, carbon dioxide (produced or injected for secondary

recovery), chlorine ion and other corrosive medium can cause serious corrosion problems which could result in huge economic losses [7,8,9]. Compared with other anticorrosion means, because the advantages of low dosage, low cost, the use of corrosion inhibitors became more common methods for corrosion protection [10]. However, the problem with chemical synthetic corrosion inhibitor is expensive, do harm to the human body in the process of production or use and can cause serious environmental problems [11].

Recently, because of its cheap, accessible, green, nontoxic and biodegradable characteristics, plant extracts use as corrosion inhibitors have received extensive attention of the scientific community. Nowadays, there have been many reports of plant extracts as corrosion inhibitors, such as bamboo leave [12], Ginkgo biloba [13,14], Phyllanthusamarus [15], Berberine [16], rice bran [17], Zanthoxylum schinifolium [18], Marigold flower [19], Parthenium hysterophorus [20], Palicourea guianensis [21], licorice [22], orange peel [23], Lupine [24], Mansoa alliacea [25], coffee [26], AzadirachtaIndica [27], Osmanthusfragran [28], Musa paradisica peel [29], Schinopsis lorentzii [30], Phoenix dactylifera L [31], Nauclea latifolia [32], etc. The plant extracts mostly contains N, O, S atomic heterocyclic compound, or polar groups, these contain lone pair electrons of the atoms or groups that can interact with charged parts of the metal surface, inhibiting the corrosion of metal.

Ilex kudingcha C.J. Tseng (Kudingcha, KDC) was also named large leaved Kudingcha, a plant that is widely distributed in southern of china. KDC has been consumed for approximately 2000 years as a traditional medicinal herbal beverage in china to antioxidants, improve eyesight, quench thirst, antihypertensive, Anti-cancer, Anti-inflammatory, clears summer-heat, refresh the mind, ect [33-37]. KDC contains numerous naturally environmental organic compounds, for instances, aponin, amino acids, alkaloid, polyphenols, flavonoids, triterpenoid, which may be utilized as environment friendly corrosion inhibitors.

Through literature retrieval we discovered that there were no reports on KDC being used as corrosion inhibitor. This motivated us for the present study to examine the inhibitive effect of the KDC plant's extract. Corrosion inhibition efficiency is examined by electrochemical techniques, using J55 steel in 3.5wt% NaCl solution saturated with CO₂. Simultaneously, Infrared Spectroscopy (IR), Scanning Electrochemical Microscopy (SECM) and scanning electron microscopy (SEM) was also use in the study.

2. EXPERIMENTAL

2.1 Specimen

J55 steel was purchased and analysed in Shengxin technology co., LTD, Shandong province, China. The experiments were conducted by J55 steel have the following composition (wt.%): C 0.24%, Si 0.22%, Mn 1.1%, P 0.103%, S 0.004%, Cr 0.5%, Ni 0.28%, Mo 0.021%, Cu 0.019% and Fe balance. which is according to the Chinese oil and gas industry standards GB/19830-2011).

2.2 Preparation of plant extract

Plant of KDC was purchased in Sichuan, China. Dried KDC were ground into powder, 20g sample of powder was soaked in 400 ml absolute ethanol for 24 h at room temperature, and then the solution was refluxed at 75°C for 4 h. The refluxed solution was filtered and concentrated to 100 ml. This solution was used to study the corrosion inhibition properties.

2.3 Characterization of KDC extract

The plant extract of KDC was characterized by Fourier transform infrared spectroscopy (FTIR). FTIR mode was Nicolet 6700 connected with Omnic software, which extended from 400 to 4000 cm^{-1} , using the KBr disk technique.

2.4 Electrochemical measurements

Electrochemical measurements were carried out with a AUTOLAB PGSTAT302N electrochemical workstation, include software NOVA1.10.4 for potentiodynamic polarization and Electrochemical Impedance Spectroscopy (EIS) measurements. The electrochemical experiments was conducted under a stander three electrode cell system, where the J55 steel with an exposed area of 1.0 cm^2 was used as working electrode (WE), platinum electrode as an counter electrode (CE) and a saturated calomel electrode (SCE) as reference electrode. In order to minimize the contribution of solution ohmic resistance, the distance between the working electrode and reference electrode should be as closely as possible. Before the potentiodynamic polarization and EIS measurements all the electrochemical tests, the WE was immersed in test solution at open circuit potential (OCP) for 30 min to ensure that the electrode reached steady condition. All of the electrochemical experiments were repeated at least three times to check the reproducibility. The polarization curves were obtained at a sweep rate of 1 mV s^{-1} in the potential range of -300 mV to $+300 \text{ mV}$ relative to the open circuit potential. The inhibition efficiency (η_p) and surface coverage (θ) of the inhibitor can be use calculated by corrosion current densities using the following equation :

$$\eta_p = \frac{I_{corr}^0 - I_{corr}}{I_{corr}^0} \times 100\% \quad (1)$$

$$\theta = \frac{I_{corr}^0 - I_{corr}}{I_{corr}^0} = 1 - \frac{I_{corr}}{I_{corr}^0} \quad (2)$$

Where i_{corr}^0 and i_{corr} represent corrosion current density values before and after additions of inhibitors, respectively.

Electrochemical impedance spectroscopy (EIS) was carried out at OCP in the frequency range of 0.01 Hz~100 kHz using 10 mV amplitude signals as voltage excitation. ZSimpWin 3.10 was used for fitting all impedance data to suitable circuits. Inhibition efficiency ($\eta_E\%$) was evaluated using the relation:

$$\eta_E = \frac{R_{ct} - R_{ct}^0}{R_{ct}} \times 100\% \quad (3)$$

$$\theta = \frac{R_{ct} - R_{ct}^0}{R_{ct}} = 1 - \frac{R_{ct}^0}{R_{ct}} \quad (4)$$

Where R_{ct}^0 and R_{ct} are charge transfer resistance for J55 steel in the absence and presence of inhibitor, respectively.

2.5 Scanning Electrochemical Microscopy (SECM)

The scanning electrochemical microscopy experiments were performed by using a model of CHI900C electrochemical system. The instrument was operated with a 10 μm platinum tip as the probe, an Ag/AgCl/KCl (saturated) reference electrode and a platinum counter electrode. The tip and substrate are part of an electrochemical cell. All potential values are referred to the Ag/AgCl/KCl (saturated) reference electrode. The measurements of line scans were generated with the tip at $\sim 10 \mu\text{m}$ from the specimen surface in all the cases. The Probe scanning range was $100 \times 100 \mu\text{m}$. The distance increment was 1 $\mu\text{m}/\text{step}$. The diameter of the samples was between $30 \times 3 \times 3 \text{ mm}$.

2.6 Surface Morphology

In order to observe the morphological changes (the effect of corrosion and inhibition) on the carbon steel surface of corrosive samples without and with the addition appropriate concentration of inhibitor, surface analysis was carried out. The SEM was performed by a ZEISS EV0 MA15 instrument.

3. RESULTS AND DISCUSSION

3.1 Characterization of KDC extract

The Fig.1 show FTIR spectrum of the KDC extract. The presence of different chemical bonds and absorption groups in KDC can be studied in this way. The absorption peaks at 2933.48 cm^{-1} and 2974.35 cm^{-1} can be attributed to the C-H stretching vibration of methylene and methyl group respectively[38]. The strong absorption bond at 1625.88 cm^{-1} is observed due to C=O stretching vibration. A peak at 1519.64 cm^{-1} could be assigned to N-H bending vibrations. The absorption peak at 1450.17 cm^{-1} could be corresponds to O-H bending vibrations. The peak at 1392.96 cm^{-1} is noticed due to C=C stretching vibration of aromatic ring. The C-O stretching vibration in Carboxylic acid, phenol, naphthenic hydrocarbon alcohol are found to be at 1274.46 cm^{-1} , 1164.13 cm^{-1} , 1082.41 cm^{-1} , 1045.63 cm^{-1} respectively. The C-N stretching vibration be founded at the peak of 882.18 cm^{-1} . The peak at 612.49 cm^{-1} is caused by C-H bending vibrations. This analysis results indicate that the extract of KDC contains nitrogen and oxygen atoms in functional groups (such as C=O, N-H, O-H, C-O, C-N,

C=C) and aromatic ring, which are generally considered to be the key of corrosion inhibitor to play a role. Previous study revealed that the presence of essential oils, flavonoids, triterpenoid in KDC [39]. Ye Shan [40], reported the presence of one isoflavones, three flavonols, one dihydroflavonol and one anthocyanidins, the relevant structure showed in Fig.2. All of these compound are organic compounds containing aromatic ring and C=O, O-H, C-O, C=C in their molecular structure, these functional groups we mentioned in the IR test part. Therefore, the adsorption of these compounds on the metal surface is assumed to be mostly responsible for the inhibition of the corrosion reaction [41].

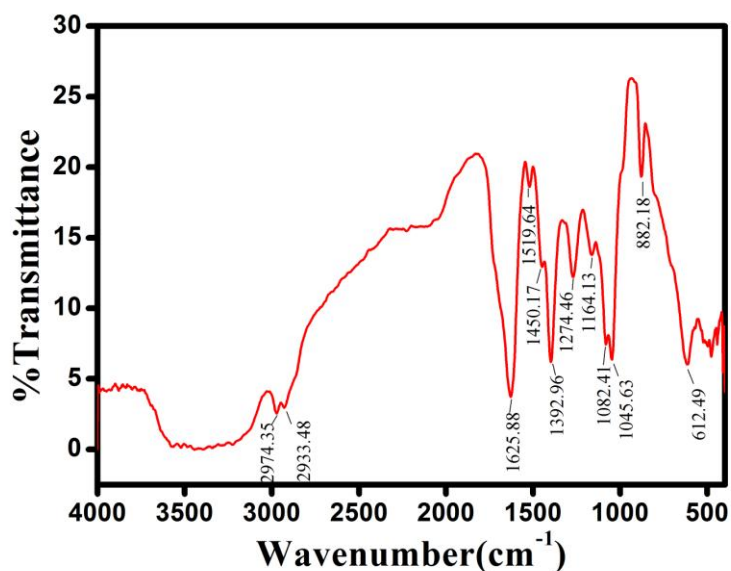


Figure 1. FTIR spectra of the KDC extract.

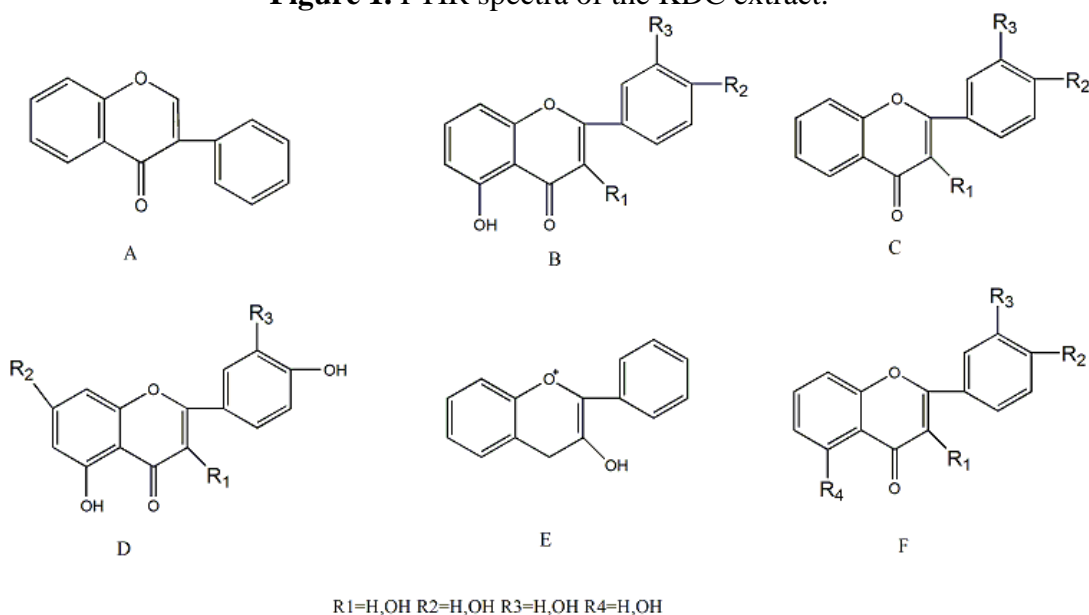


Figure 2. The chemical structures of isoflavones (A), three flavones or flavonols (B,D,F), flavanones or flavanonol (C) and anthocyanins (E).

3.2 Electrochemical impedance spectroscopy (EIS)

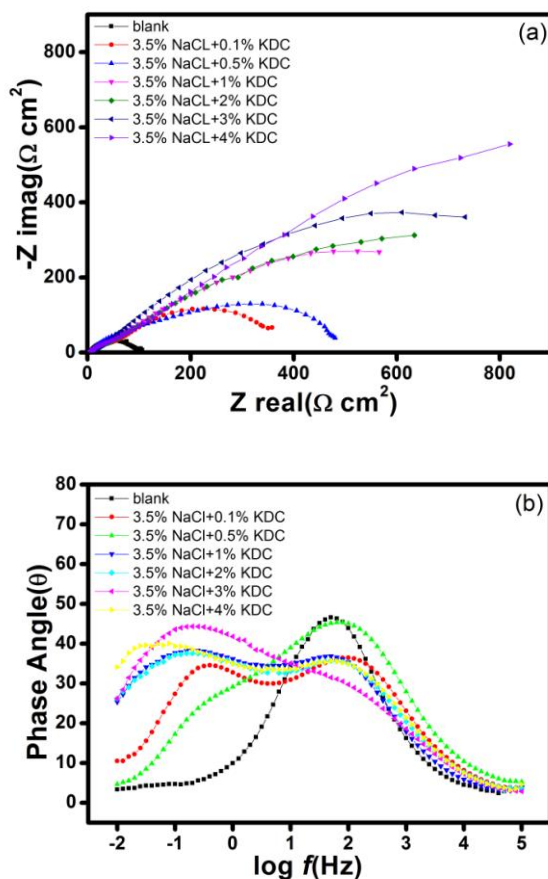


Figure 3. (a) Nyquist plot and (b) Theta-frequency plot for J55 steel in 3.5wt% NaCl saturated with CO_2 solution containing different concentration of KDC extract at 25°C .

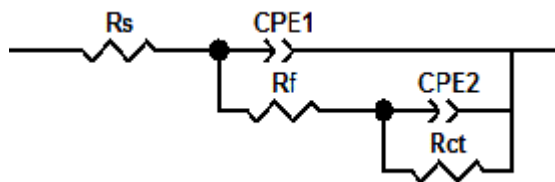


Figure 4. The equivalent circuit used for fit the impedance data, record for J55 steel in 3.5% NaCl saturated with CO_2 solution in the presence of KDC extract.

The corrosion behavior of J55 steel in 3.5wt% NaCl saturated with CO_2 in the presence and absence of different concentrations of KDC was investigated by EIS. Fig.3a and 3b illustrate the Nyquist plots and Theta-frequency, respectively. It can be observed that the impedance response behavior of J55 steel shows significant change after the addition of KDC extract in test solution. For sample in the solution without inhibitor, it only observed one peak in the phase angle vs. frequency plot and there was one capacitive loop in Nyquist plot. This result cleared that there was only one time constant, the system could be described by the equivalent circuit shown in Fig.3. While when

corrosion inhibitor was added into the solution, there were two peaks in angle vs. frequency plot and also two capacitive loops has been observed, at high frequency which can be assigned to the relaxation process of corrosion inhibitor molecular film presents on the J55 steel surface, the low frequency capacitive loop was assigned to the Faradic charge transfer process of the metal dissolution [42] and comparison of the radii of the capacitive loops of the J55 steel in blank solution and that in the presence of the different concentrations of KDC shows that the real axis intercepts at low frequencies in the presence of the inhibitor is larger than those in the absence of the inhibitor and increase as the inhibitor concentration increases. This confirms that the impedance of J55 steel increases with the concentration of KDC in 3.5wt% NaCl solution. Fig.4a also clear shows that these EIS spectra are not perfect semicircle, such behavior often relate with nonhomogeneity, the rough-textured metal surface or adsorption of the inhibitor molecules [43,44]. The effectiveness of KDC can be attributed to adsorption of its main constituent flavonoid substances at the metal solution interface. These compounds may be adsorbed by the interaction between either the lone pairs of electrons on oxygen atoms or conjugated double bond or both present in flavonoid as well as protonated flavonoid and the vacant d-orbital of iron in mild steel [45]. The increase in inhibition efficiency with concentration of KDC is because of the availability of larger number of molecules in both the forms for adsorption at higher concentrations. An equivalent circuit was introduced to fitting the impedance spectra for Nyquist plots as show in Fig.4 [46], Where R_s is the solution resistance, $CPE1$ is the film capacity, R_f is the film resistance, $CPE2$ is the double layer capacity, R_{ct} is the charge transfer resistance.

The electrochemical impedance parameters such as solution resistance (R_s), charge transfer resistance (R_{ct}), phase shift (n), and inhibition efficiency ($\eta\%$), are listed in table 1. It is clearly seen from the result that R_{ct} increases with the concentration of KDC increasing. Usually, the increase of R_{ct} value represent the reaction of CO_2 corrosion were inhibited [47]. The greatest corrosion inhibition efficiency exhibited by the KDC extract for J55 steel corrosion in test solution was 92.65%. The above result confirms that KDC have a good inhibition effect in 3.5wt% NaCl saturate CO_2 solution at room temperature.

Table 1. EIS parameters for J55 steel in 3.5wt% NaCl saturated with CO_2 solution in the absence and presence of KDC extract.

Concentration (%v/v)	R_s (Ωcm^{-2})	$10^4 Y_{CPE1}$ ($S cm^{-2} s^{-n}$)	R_f (Ωcm^{-2})	$10^4 Y_{CPE2}$ ($S cm^{-2} s^{-n}$)	n	R_{ct} (Ωcm^{-2})	η (%)
blank	5.771	-	-	5.726	0.7632	95.35	-
0.1	5.310	9.34	77.82	33.53	0.7383	324.5	70.62
0.5	5.461	5.939	79.92	21.89	0.7672	480.1	80.76
1	5.365	12.34	64.60	40.42	0.5790	1080	91.17
2	5.858	11.36	76.87	34.48	0.5749	1190	91.99
3	5.516	21.78	73.98	17.29	0.6583	1579	94.09
4	6.029	11.71	99.22	32.77	0.5768	2755	96.53

3.3 Potentiodynamic polarization curves

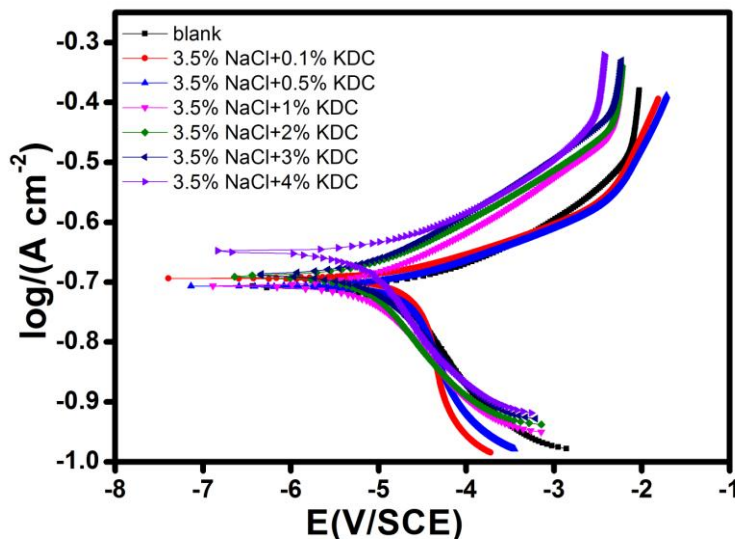


Figure 5. Polarization curves for J55 steel in 3.5wt% NaCl saturated with CO₂ solution containing different concentration of KDC extract at 25 °C.

Fig.5 shown the potentiodynamic polarization curves for J55 steel at different concentration of KDC in 3.5wt% NaCl solution saturated with CO₂. The relevant electrochemical parameters of the corrosion potential (E_{corr}), the corrosion current density (I_{corr}), the anodic slope (β_a) and cathodic slope (β_c), inhibition efficiency(η) and surface coverage (θ) are shown in Table.2. It can observe from Fig.6 that the presence of extract have a minimal effect on cathodic slope, the small change in cathodic tafel slopes show that the addition of the KDC extract does not modify the mechanism of cathodic process [48]. For the changes in anodic slopes, that might be due to the chloride ions or inhibitor molecules being absorbed on metal surface [49,28].

Table 2. Polarization parameters and corresponding inhibition efficiency for J55 steel in 3.5wt% NaCl saturate with different concentration of KDC extract.

Concentration (%v/v)	$-E_{\text{corr}}$ vs. SCE (mv)	I_{corr} (μAcm^{-2})	β_a (mV dec^{-1})	β_c (mV dec^{-1})	Corrosion rate (mm y^{-1})	η (%)	Surface coverage (θ)
blank	712	35.986	195.440	77.843	0.4178	-	-
0.1	694	11.749	202.561	80.582	0.1748	67.35	0.6735
0.5	705	8.910	197.659	73.238	0.1136	75.24	0.7524
1	706	7.0052	151.460	63.919	0.0812	80.52	0.8052
2	690	5.7094	180.530	55.269	0.0663	86.91	0.8691
3	687	3.5194	171.180	63.323	0.0409	90.22	0.9022
4	668	1.1755	192.692	65.390	0.0137	92.65	0.9265

Table.2 data clearly illustrate that with the concentration of KDC inhibitor increasing, the corrosion current density decreased, the inhibition efficiency and surface coverage increased. This result confirmed the good inhibitive effect of KDC toward corrosion of the J55 steel, which is in agreement with EIS test result. This table shows that the corrosion potential values was shifted to the positive values in the presence of the KDC extract (from -712 mV to -668 mV), but has not been changed significantly. This effect may be related to the adsorption of the organic compound at the active sites of the electrode surface, retarding the corrosion reaction [50]. Further, it can be seen from these potentiodynamic polarization results in Table 2 that the corrosion current density and corrosion rate decreases noticeably and the $\eta\%$ increases with the concentration of KDC. Tafel slope constants (β_a and β_c) do not change significantly in inhibited system as compared to uninhibited system. This suggests that inhibitor does not participate in the mechanism of corrosion [51]. Usually, an inhibitor can be classified as anodic or cathodic type if the shift of corrosion potential with the inhibitor is more than 85 mV with respect to that without the inhibitor [52]. In the presence of inhibitor, the change of E_{corr} is 6-44 mV, which indicate that KDC extract acts as a mixed-type inhibitor for the corrosion of J55 steel in 3.5% NaCl solution saturate with CO_2 . This also indicates that the dissolution of the metal is reduced and the hydrogen evolution reaction is diminished by the blocking effect of KDC on J55 steel surface.

3.4 Adsorption isotherm

The mechanism of inhibition reaction can be study by the evaluation of adsorption isotherm. The interaction of inhibitor molecules on the metal surface can be studied by investigating the mode of adsorption and the adsorption isotherm. The data obtain from potentiodynamic polarization and EIS study have been use to explain the best isotherm to determine the inhibitor adsorption behaviors. Langmuir, Frumkin and Temkin isotherms were used to fit the experiment data. Those relevant adsorption isotherms can be express by following equations [53]:

$$\frac{C_{\text{inh}}}{\theta} = \frac{1}{K_{\text{ads}}} + C_{\text{inh}} \text{ (Langmuir isotherm)} \quad (5)$$

$$\left(\frac{\theta}{1-\theta}\right) \exp(-2a\theta) = K_{\text{ads}} C_{\text{inh}} \text{ (Frumkin isotherm)} \quad (6)$$

$$\exp(-2a\theta) = K_{\text{ads}} C_{\text{inh}} \text{ (Temkin isotherm)} \quad (7)$$

Where θ is the degree of surface coverage, K_{ads} is the equilibrium constant of absorption, C_{inh} is the inhibitor concentration and a is the parameter of interaction between inhibitor molecules adsorbed on the steel surface.

By plot C_{inh}/θ versus θ , $\ln[C_{\text{inh}}(1-\theta)/\theta]$ versus θ and θ versus $\ln C_{\text{inh}}$, Langmuir, Frumkin and Temkin adsorption isotherm plot were obtained (Fig 6). It can be seem from the picture that only the Langmuir adsorption plots both has higher linear correlation coefficients when Tafel and EIS data are use [54]. The best straight line is obtained with correlation coefficient (R^2) 0.99873 for EIS and 0.99847 for Tafel, which indicated that KDC extract as inhibitor follow Langmuir adsorption isotherm [16,49,55]. The slopes are very close to 1, suggesting that adsorbed inhibitor molecules form

monolayer on the metal surface and there is no interaction among the adsorbed inhibitor molecules [56].

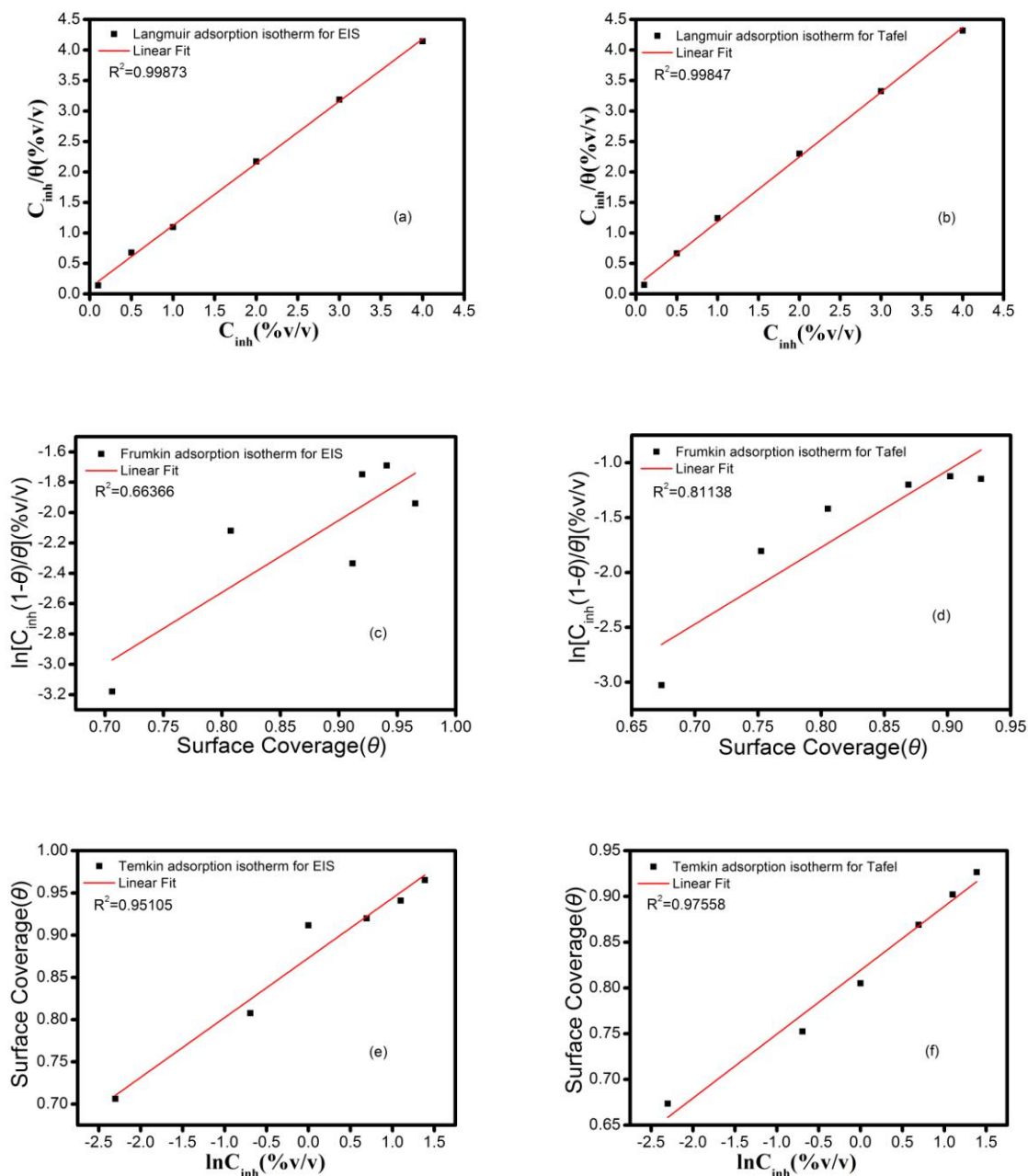
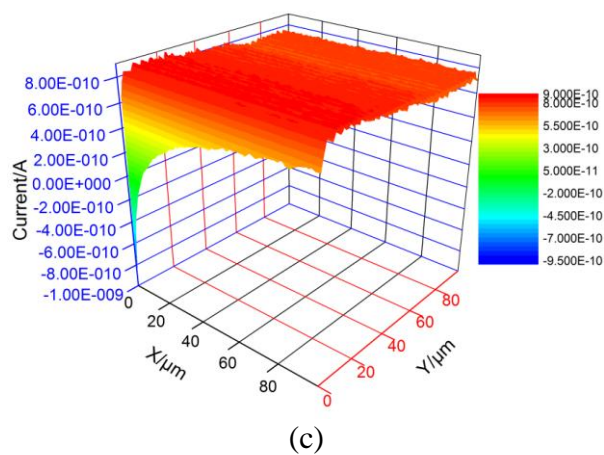
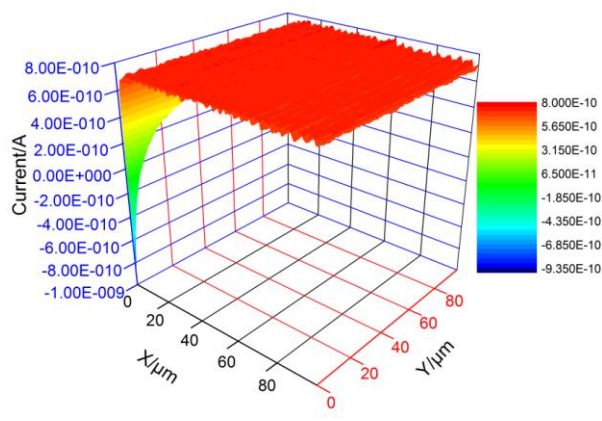
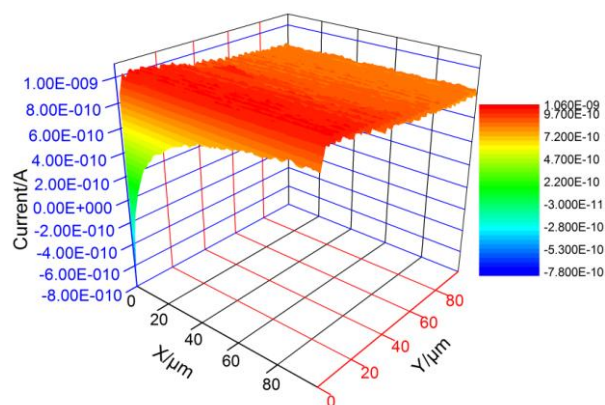


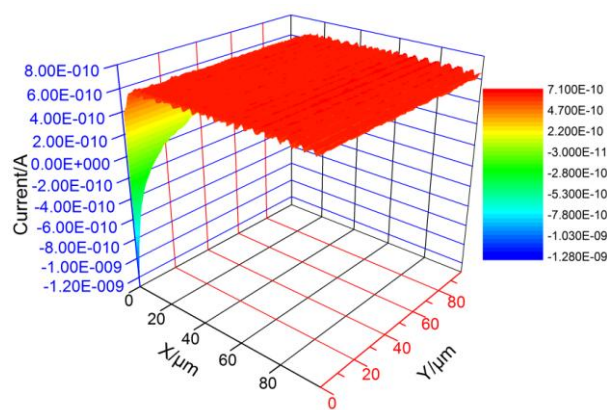
Figure 6. The adsorption isotherm plots for (a) Langmuir EIS (b) Langmuir Tafel (c) Frumkin EIS (d) Frumkin Tafel (e) Temkin EIS and (f) Temkin Tafel at different concentrations of KDC.

3.5 Scanning Electrochemical Microscopy (SECM)

Scanning electrochemical microscope (SECM) is a very useful technique for characterizing local electrochemical activity and pitting at films [57]. Fig. 7a-d shows the morphology of the samples as observed under SECM in presence and absence of KDC. The distance between the probe and the sample was established by approach curves prior to each experiment. It can be seen that when KDC

has been added to the test solution the tip current became more smaller [58]. According to Singh [59] study, when an insulating surface covering the steel surface is approached by the probe, there is hindrance in the diffusion current and the tip current decreases. On the contrary, an increase in the current is observed when a conductor surface is approached, because the redox mediator is regenerated at the surface. Comparing the currents across the corroded sample (absence KDC inhibitor) and the specimens incorporated with inhibitor solution, the inhibitor adsorbed on J55 steel surface can be proved [13,60].



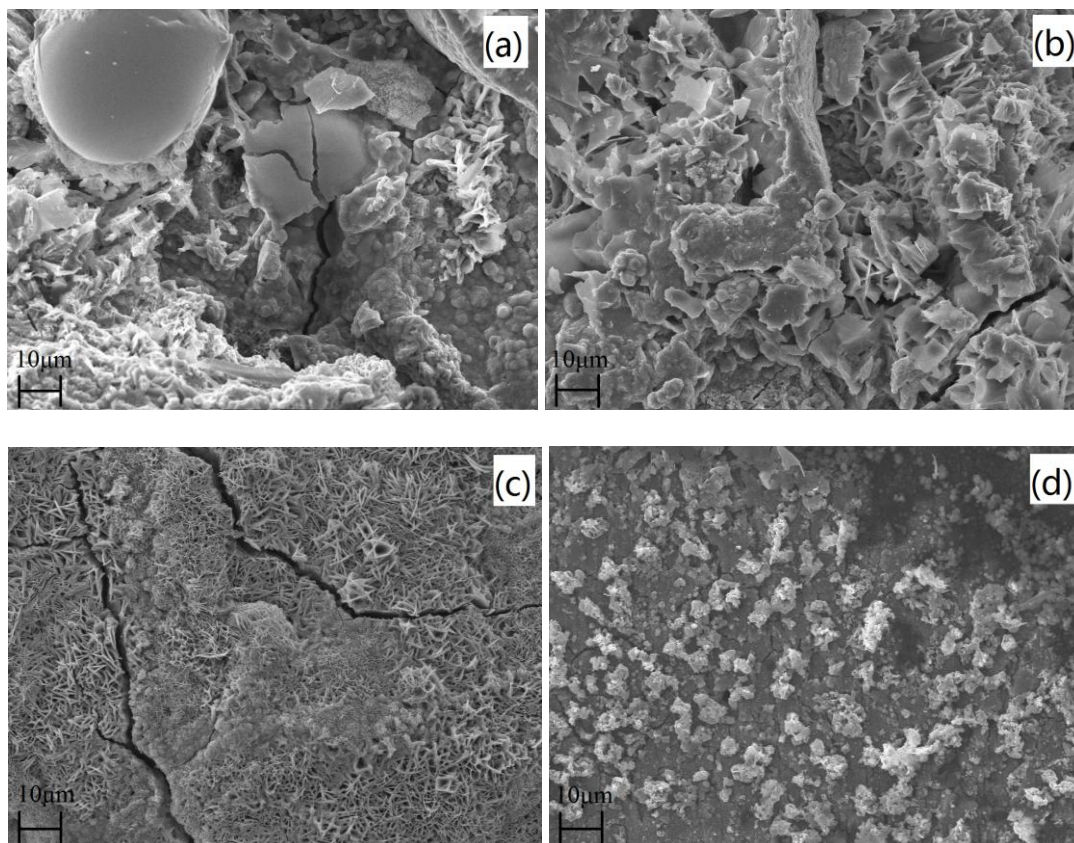


(d)

Figure 7. SECM figures for (a) 3.5% NaCl x axis (b) 3.5% NaCl y axis (c) 4% KDC x axis and (d) 4% KDC y axis.

3.6 Surface analysis

The surface morphologies of the J55 steel specimens used for electrochemical experiments with and without KDC inhibitor were examined by scanning electron microscope (SEM), the corresponding images are shown in Fig.8.



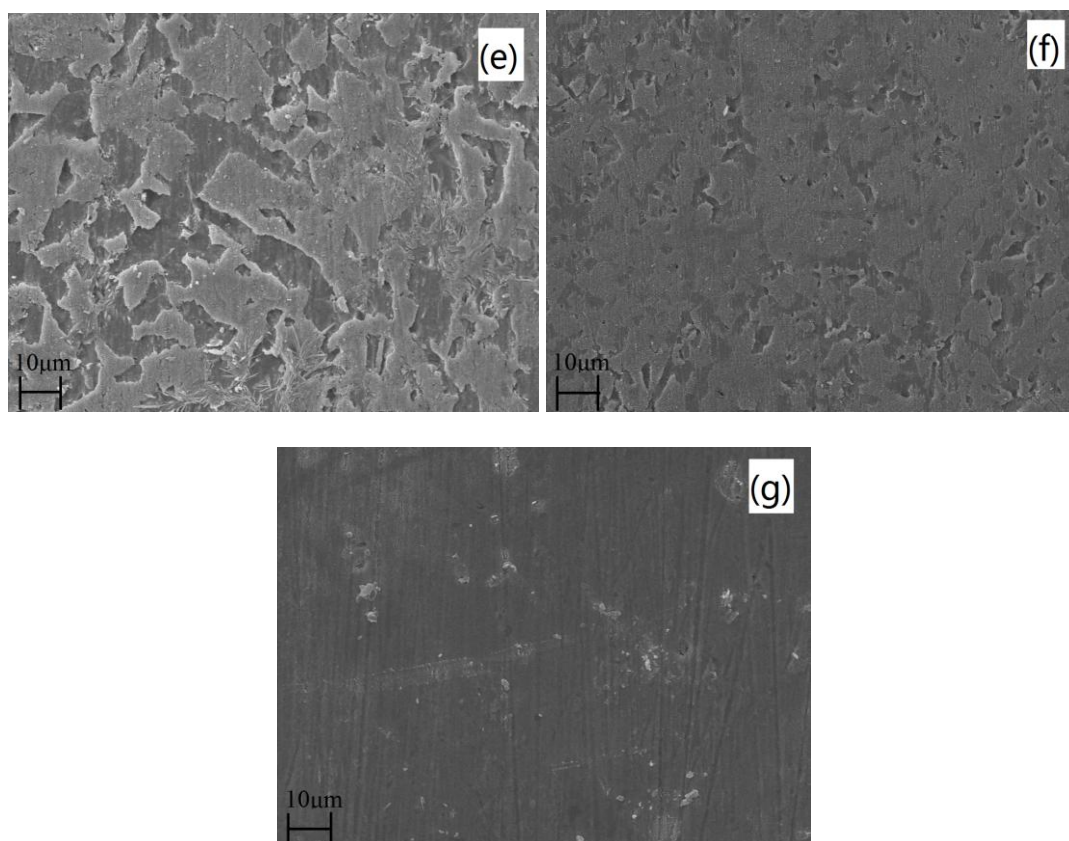


Figure 8. SEM micrographs of J55 steel in (a) 3.5 % NaCl (b) 0.1% KDC (c) 0.5% KDC (d) 1% KDC (e) 2% KDC (f) 3% KDC (g) 4% KDC.

It can be seen from the diagram that corrosion was serious for the steel sample exposed in the corrosion solution without inhibitor (Fig.8a). But, when inhibitor was introduced to the system, a smooth and less corroded morphology was obtained, especially in in Fig.8f and g, which could be ascribed to a protective layer was formed of J55 steel surface. All of these result proved that KDC inhibitor can effectively protect J55 steel in 3.5wt% NaCl saturated with CO₂ solution. These results are consistent with electrochemical and adsorption experiments results.

4. CONCLUSIONS

In this study, corrosion inhibition efficiency of KDC on J55 steel in 3.5% NaCl solution saturated with CO₂ was determined by electrochemical and surface analysis. Potentiodynamic

polarization curves illustrated that KDC inhibitor acted as mixed-type inhibitor and didn't modify the mechanism of cathodic hydrogen evolution reaction. Inhibition efficiency value increases with increasing the inhibitor concentration, the inhibitor showed maximum inhibition efficiency up to 96.53% at 4% inhibitor concentration in EIS study. The adsorption behavior of KDC inhibitor on J55 steel in test solution obeyed Langmuir adsorption isotherm. The surface studies by scanning electrochemical spectroscopy confirmed the blockage of metal surface through adsorption process. SEM and SECM results clearly showed that KDC inhibit J55 steel corrosion by formation a protective

film on the steel surface and a significant decrease of corrosion is observed when inhibitor is added into the system. All these data support KDC extract acts as a good inhibitor for J55 steel in 3.5wt% NaCl solution saturate with CO₂.

ACKNOWLEDGEMENTS

Authors are thankful for the financial assistance provided by the National Natural Science Foundation of China (No. 51274170), Key Laboratory of Oil and Gas Fields materials Open Fund of Sichuan Province (No.X151516KCL47).

References

1. G. Ji, S. K. Shukla, P. Dwivedi, S. Sundaram and R. Prakash, *Ind. Eng. Chem. Res.*, 50 (2011) 11954.
2. R. Javaherdashti, *Anti-corros. Meth. Mater.*, 47 (2000) 30.
3. K. S. Ventakeshwarlu, *Corros. Maint.*, 2 (1979) 257.
4. F.C.R. Hernández, G. Plascencia and K. Koch, *Eng. Fail. Anal.*, 16 (2009) 281.
5. L. Ni, A. Chemtob, N. Moreau, T. Boudier, S. Chanfreau and N. Pébère, *Corros. Sci.*, 89 (2014) 242.
6. J. Bhandari, F. Khan, R. Abbassi, V. Garaniya and R. Ojeda, *J. Loss. Prevent. Pro. Ind.*, 37 (2015) 39.
7. A. Singh, Y. Lin, E. E. Ebenso, W. Liu, J. Pan and B. Huang, *J. Ind. Eng. Chem.*, 24 (2015) 219.
8. C. H. Peng, Z. Y. Liu. and X. Z. Wei, *Eng. Fail. Anal.*, 25 (2012) 13.
9. D. Brondel, F. Montrouge, R. Edwards, A. Hayman, D. Hil, S. Mehta and T. Semerad, *J. Petro. Tech.*, 39 (1987) 756.
10. P. B. Raja and M. G. Sethuraman, *Mat. Lett.*, 62 (2008) 113.
11. M. M. Solomon, S. A. Umoren, I. I. Udosoro and A. P. Udoh, *Corros. Sci.*, 52 (2010) 1317.
12. L. Li, X. Zhang, J. Lei, J. He, S. Zhang and F. Pan, *Corros. Sci.*, 63 (2012) 82.
13. A. Singh, Y. Lin., E.E. Ebenso, W. Liu and B. Huang, *Int. J. Electrochem. Sci.*, 9 (2014) 5993.
14. G. Chen, M. Zhang, J. R. Zhao, Z. Meng and J. Zhang, *Chem. Central. J.*, 7 (2013) 1.
15. P. C. Okafor, M. E. Ikpi, I. E. Uwah, E. E. Ebenso, U. J. Ekpe and S. A. Umoren, *Corros. Sci.*, 50 (2008) 2310.
16. Y. Lin, A. Singh, E. E. Ebenso, M. A. Quraishi, Y. Zhou and Y. Huang, *Int. J. Electrochem. Sci.*, 10 (2015) 194.
17. D. Liu, Y. H. Lin, Y. G. Ding and D. Z. Zeng, *Anti. Corros. Meth. Mater.*, 58 (2011) 205.
18. A. Singh, Y. H. Lin, E. E. Ebenso, W. Y. Liu, K. H. Deng, J. Pan and H. Bo, *Int. J. Electrochem. Sci.*, 9 (2014) 5585.
19. P. Mourya, S. Banerjee and M. M. Singh, *Corros. Sci.*, 85 (2014) 352.
20. G. Ji, S. K. Shukla, P. D. wivedi, S. Sundaram, E. E. Ebenso and R. Prakash, *Int. J. Electrochem. Sci.*, 7 (2012) 9933.
21. M. Lebrini., F. Robert and C. Roos, *Int. J. Electrochem.*, 6 (2011) 847.
22. M. A. Deyab, *J. Ind. Eng. Chem.*, 22 (2015) 384.
23. N. M'hiri, D. Veys-Renaux, E. Rocca, I. Ioannou, N. M. Boudhrioua and M. Ghoul, *Corros. Sci.*, 102 (2016) 55.
24. A. M. Abdel-Gaber, B. A. Abd-El-Nabey and M. Saadawy, *Corros. Sci.*, 51 (2009) 1038.
25. F. Suedile, F. Robert, C. Roos and M. Lebrini, *Electrochim. Acta.*, 133 (2014) 631.
26. V. V. Torres, R. S. Amado, C. F. de Sá, T. L. Fernandez, C. A. da Silva Riehl, A. G. Torres and E. D'Elia, *Corros. Sci.*, 53 (2011) 2385.
27. P. C. Okafor, E. E. Ebenso and J. E. Udofot, *Int. J. Electrochem. Sci.*, 5 (2010) 978.

28. X. Li, S. Deng and H. Fu, *Corros. Sci.*, 62 (2012) 163.
29. G. Ji, S. Anjum, S. Sundaram and R. Prakash, *Corros. Sci.*, 90 (2015) 107.
30. H. Gerengi and H. I. Sahin, *Ind. Eng. Chem. Res.*, 51 (2011) 780.
31. H. Gerengi, *Ind. Eng. Chem. Res.*, 51 (2012) 12835.
32. I. E. Uwah, P. C. Okafor and V. E. Ebiekpe, *Arab. J. Chem.*, 6 (2013) 285.
33. D. Xu, Q. Wang, W. Zhang, B. Hu, L. Zhou, X. Zeng and Y. Sun, *J. Agric. Food. Chem.*, 63 (2015) 3694.
34. F. Zhu, Y. Z. Cai, M. Sun, J. Ke, D. Lu and H. Corke, *J. Agric. Food. Chem.*, 57 (2009) 6082.
35. Z. Y. Chen, I. Y. F. Wong, M. W. S. Leung, Z. D. He and Y. Huang, *J. Agric. Food. Chem.*, 50 (2002) 7530.
36. K. Zhu, G. Li, P. Sun, R. Wang, Y. Qian and X. Zhao, *Exp. Ther. Med.*, 7 (2014) 709.
37. J. L. Song, Y. Qian, G. Li. J and X. Zhao, *Mol. Med. Rep.*, 8 (2013) 1256.
38. M. Jokar, T. S. Farahani and B. Ramezanzadeh, *J. Taiwan. Inst. Chem. Eng.*, 63 (2016) 436.
39. L. Li, L. J. Xu., G. Z. Ma, Y. M. Dong, Y. Peng and P. G. Xiao, *J. Nat. Med.*, 67 (2013) 425.
40. S. R. Ye, Q. Tang and X. Du, *Sichuan. Agric. Univ.*, 22 (2004) 157.
41. G. Ji, S. Anjum, S. Sundaram, and R. Prakash, *Corros. Sci.*, 90(2015)107.
42. M. Álvarez., Rodolfo, C. J. Mendoza, C. S. Castillo and C. J. Marín, *J. Mex. Chem. Soc.*, 57 (2013) 30.
43. A. Singh., Y. H. Lin, W. Y. Liu, D. Kuanhai, J. Pan, B. Huang and D. Z. Zeng, *J. Taiwan. Inst. Chem. Eng.*, 45 (2014) 1918.
44. S. K. Shukla and M. A. Quraishi, *Corros. Sci.*, 51 (2009) 1990.
45. A. K. Satapathy , G. Gunasekaran, S. C. Sahoo, K. Amit and P. V. Rodrigues, *Corros. Sci.*, 51(2009) 2848.
46. M. Mishra, K. Tiwari, A. K. Singh, V. P. Singh, M. Mishra and K. Tiwari, *Polyhedron*, 77 (2014) 57.
47. M. N. El-Haddad and A. S. Fouda, *J. Mol. Liq.*, 209 (2015) 480.
48. K. F. Khaled and M. M. Al-Qahtani, *Mater. Chem. Phys.*, 113 (2009) 150.
49. Y. Yan, W. Li, L. Cai and B. Hou, *Electrochim. Acta.*, 53 (2008) 5953.
50. F. Suedile, F. Robert, C. Roos, and M. Lebrini, *Electrochim. Acta.*, 133(2104) 631.
51. M. A. Deyab, *J. Taiwan. Inst. Chem. Eng.*, 58 (2015) 536.
52. T. Peme, L. O. Olasunkanmi, I. Bahadur, A. S. Adekunle, M. M. Kabanda and E. E. Ebenso, *Mol.*, 20 (2015) , 16004.
53. A. K. Satapathy, G. Gunasekaran, S. C. Sahoo, K. Amit and P. V. Rodrigues, *Corros. Sci.*, 51 (2009) 2848.
54. L. R. Chauhan and G. Gunasekaran, *Corros. Sci.*, 49(2007) 1143.
55. A. S. Yaro, A. A. Khadom and R. K. Wael, *Alexandria. Eng. J.*, 52(2013) 129.
56. W. Liu, A. Singh, , Y. Lin, E. E. Ebenso, L. Zhou and B. Huang, *Int. J. Electrochem. Sci.*, 9 (2014) 5574.
57. H. Zarrok, A. Zarrouk, R. Salghi, H. Oudda, B. Hammouti and M. E. Touhami, *Port. Electrochim. Acta.*, 30(2012)405.
58. A. Singh, Y. Lin, W. Liu, S. Yu, J. Pan and C. Ren, *J. Ind. Eng Chem.*, 20 (2014) 4276.
59. A. Singh, Y. Lin, E. E. Ebenso, W. Liu and B. Huang, *Int. J. Electrochem. Sci.*, 10 (2015) 6900.
60. B. M. Quinn, I. Prieto, S. K. Haram and A. J. Bard, *J. Phys. Chem. B.*, 105(2001)7474.